

Title: Phase analysis in maximal sprinting: an investigation of step-to-step technical changes between the initial acceleration, transition and maximal velocity phases.

Authors:

Hans C. von Lieres und Wilkau¹, Gareth Irwin¹, Neil E. Bezodis², Scott Simpson³, Ian N. Bezodis¹

Cardiff School of Sport and Health Sciences, Cardiff Metropolitan University, Cardiff, Wales, UK¹

Applied Sports, Technology, Exercise and Medicine Research Centre, Swansea University, Swansea, Wales, UK²

Welsh Athletics, Cardiff, Wales, UK³

Correspondence:

Hans C. von Lieres und Wilkau, Cardiff School of Sport and Health Sciences, Cardiff Metropolitan University, Cardiff, Wales, UK. E-mail: havonlieres@cardiffmet.ac.uk, Telephone number: 029 2020 5027.

Co-authors:

Gareth Irwin, Cardiff School of Sport and Health Sciences, Cardiff Metropolitan University, Cardiff, Wales, UK. girwin@cardiffmet.ac.uk, Telephone number: 029 2041 7274.

Neil E. Bezodis, Applied Sports, Technology, Exercise and Medicine Research Centre, Swansea University, Swansea, Wales, UK. n.e.bezodis@swansea.ac.uk, Telephone number: (01792) 295801.

Scott Simpson, Welsh Athletics, Cardiff, Wales, UK, scott.simpson@welshathletics.org, Telephone number: 029 2020 1520.

Ian N. Bezodis, Cardiff School of Sport and Health Sciences, Cardiff Metropolitan University, Cyncoed Road, Cardiff, Wales, UK. ibezodis@cardiffmet.ac.uk, 029 2041 7245.

Acknowledgements:

The authors are grateful to Melanie Golding, Laurie Needham, Adam Brazil and James Cowburn for their assistance with data collection, and to the coach and athletes who participated in this study.

Funding:

This work was supported by Welsh Athletics, Sport Wales and the Cardiff School of Sport and Health Sciences.

1 **Abstract**

2 The aim of this study was to investigate spatiotemporal and kinematic changes between the
3 initial acceleration, transition and maximum velocity phases of a sprint. Sagittal plane
4 kinematics from five experienced sprinters performing 50 m maximal sprints were collected
5 using six HD-video cameras. Following manual digitising, spatiotemporal and kinematic
6 variables at touchdown and toe-off were calculated. The start and end of the transition phase
7 were identified using the step-to-step changes in centre of mass height and segment angles.
8 Mean step-to-step changes of spatiotemporal and kinematic variables during each phase were
9 calculated. Firstly, the study showed that if sufficient trials are available, step-to-step changes
10 in shank and trunk angles might provide an appropriate measure to detect sprint phases in
11 applied settings. However, given that changes in centre of mass height represent a more
12 holistic measure, this was used to sub-divide the sprints into separate phases. Secondly,
13 during the initial acceleration phase large step-to-step changes in touchdown kinematics were
14 observed compared to the transition phase. At toe-off, step-to-step kinematic changes were
15 consistent across the initial acceleration and transition phases before plateauing during the
16 maximal velocity phase. These results provide coaches and practitioners with valuable
17 insights into key differences between phases in maximal sprinting.

18

19 Key Words: acceleration phase; kinematics; sprint technique; coaching

20

21

22

23

24

25

26 **Introduction**

27 The sprint running events have traditionally been sub-divided into acceleration, constant
28 velocity and deceleration phases (e.g. Volkov & Lapin, 1979). Due to the multidimensional
29 structure of the acceleration phase (Delecluse, 1997), the scientific (e.g. Delecluse, Van
30 Coppenolle, Willems, Diels, Goris, Van Leemputte & Vuylsteke, 1995; Čoh & Tomazin, 2006;
31 Nagahara, Matsubayashi, Matsuo & Zushi, 2014b) and coaching (e.g. Dick, 1989; Seagrave,
32 1996; Crick, 2014a) literature have further sub-divided the acceleration phase. For the purposes
33 of this paper, the naming convention used by Delecluse et al. (1995) will be adopted, where the
34 first and second acceleration phases will be referred to as the initial acceleration phase and the
35 transition phase, respectively. The transition phase is then followed by the maximal velocity
36 phase.

37

38 With performance-related factors differing between the phases in a sprint, Delecluse, Van
39 Coppenolle, Diels and Goris (1992) suggested that a good performance in one phase does not
40 guarantee good performance in other phases. An increased understanding of the characteristics
41 of the different phases in sprinting can provide important insights for coaches and applied sport
42 scientists of the changes in mechanics between phases of a maximal sprint. However, with the
43 specific length of each phase dependent on the athletes' ability (Delecluse, 1997), it is
44 challenging to tailor training sessions to individual athletes. Recently, scientific (e.g. Nagahara
45 et al., 2014b) and coaching literature (e.g. Crick, 2014a) identified the use of step-to-step
46 progressions of postural measures to identify phases in maximal sprinting.

47

48 Using the step-to-step changes of the centre of mass height (CM-h), Nagahara et al. (2014b)
49 identified two breakpoint steps (approximately steps 4 and 14) which were used to subdivide
50 the sprint into three phases. Distinct changes were reported in spatiotemporal and kinematic

51 variables (Nagahara et al., 2014b) and external kinetics (Nagahara, Mizutani & Matsuo, 2016;
52 Nagahara, Mizutani, Matsuo, Kanehisa & Fukunaga, 2018a) as sprinters crossed from one
53 phase to the next. Similarly, coaching literature proposed that step-to-step progressions of shank
54 and trunk angles at touchdown are specific to each phase of a maximal sprint (Crick, 2014a). It
55 is suggested that the initial acceleration phase ends when step-to-step changes in shank angles
56 end as the shank becomes perpendicular to the ground at touchdown (suggested to be: steps 5-
57 7; Crick, 2014b), while the transition phase ends when step-to-step changes in trunk angle cease
58 as the trunk becomes upright (suggested to be: step 17; Crick, 2014c). However, considering
59 that changes in CM-h represent a holistic measure of whole-body changes it is unknown
60 whether the first and second acceleration phases identified by Nagahara et al. (2014b) will align
61 with the initial acceleration and transition phases described by Crick (2014a). This may have
62 important practical implications to ensure the appropriate alignment of information that is
63 shared between researchers, coaches and applied sport scientists.

64

65 Performance during sprint acceleration depends on the net anteroposterior force generated
66 during ground contact, which directly influences the anteroposterior centre of mass (CM)
67 acceleration (Rabita, Dorel, Slawinski, Sàez de Villarreal, Couturier, Samozino & Morin,
68 2015). Theoretically, the orientation of the sprinter (i.e. the vector connecting the sprinter's CM
69 to the contact point with the ground (CM-angle) is mechanically related to their acceleration (di
70 Prampero, Fusi, Sepulcri, Morin, Belli & Antonutto, 2005). As sprinters assume a more
71 forward-inclined CM-angle during the initial acceleration phase, anteroposterior CM
72 acceleration is larger compared with the later phases of a sprint when sprinters adopt a less
73 forward-inclined posture. However, the CM-angle depends on both the CM-h and the
74 anteroposterior distance between the contact point and the CM, which in turn are dependent on
75 the orientation of the segments of the stance leg and trunk. Thus, knowledge of the step-to-step

76 changes in segment angles of the stance leg and trunk are important to understand how
77 sprinters' orientation and CM acceleration changes to address the requirements of the different
78 sprint phases.

79

80 An understanding of the evolution of whole-body posture and segment orientations during
81 acceleration can have important implications for developing technical models of sprinting and
82 informing technical interventions. Therefore, the aim of this study was to investigate
83 spatiotemporal and kinematic changes between the initial acceleration, transition and maximum
84 velocity phases of a sprint. Two research questions were formulated; the first research question
85 – *'how comparable are the sprint acceleration phases when identified using different*
86 *measures?'* aimed to compare and critically appraise the use of either CM-h (Nagahara et al.,
87 2014b) or shank and trunk angles (Crick, 2014a) to identify breakpoint steps in sprint
88 acceleration. The second research question – *'how do step-to-step progressions of*
89 *spatiotemporal and kinematic variables differ between the initial acceleration, transition and*
90 *maximal velocity phases?'* aimed to characterise the technical changes throughout a maximal
91 sprint. It was hypothesised that; a) the sprint acceleration phases identified using changes in
92 CM-h will align with the phases identified using shank and trunk angles and b) there will be
93 large differences in step-to-step changes of the orientation of sprinters (i.e. CM-angle) between
94 the initial acceleration, transition and maximal velocity phases.

95

96 **Methods**

97 *Participants and procedures*

98 Following institutional ethical approval, three male and two female national-level sprinters
99 (Table 1) gave written informed consent to participate. Data were collected in March (after the

100 indoor season) and eight weeks later in May (early outdoor season) during participants' regular
101 training sessions.

102

103 ****Insert table 1 near here****

104

105 Prior to data collection, the participants performed a coach-led warm-up. The warm-up
106 incorporated; dynamic stretching, sprint specific drills, and was concluded with 3-5 runs of
107 increasing intensity. The participants then performed up to three practice starts from the starting
108 blocks, before commencing with the data collection. Following the warm-up, data were
109 collected from five maximal 50 m sprints from blocks, with at least five minutes rest between
110 trials to ensure a full recovery. One sprinter (P3) only completed three sprints at the second
111 collection. Each sprint was started with 'on your marks' and 'set' commands, followed by a
112 manually triggered auditory starting signal. All participants wore sprinting shoes and the testing
113 was done on a Mondo track surface.

114

115 *Data collection set-up*

116 Five HDV digital cameras (1×Sony Z5; 2×Sony Z1; 2×Sony A1E, Sony, Tokyo, Japan) were
117 mounted on tripods at a height of 1.80 m and 19 m from the running lane (Cameras 1 – 5; Figure
118 1). The cameras recorded in HD (1440 × 1080 pixels) at 50 Hz with an open iris and a shutter
119 speed of 1/600 s.

120

121 ****Insert figure 1 near here****

122

123 A sixth camera (Sony Z5) was set up perpendicular to the 25 m mark and 40 m away from the
124 running lane and was panned during trials and used to identify touchdown and toe-off events.

125 It recorded in HD (1440×1080 pixels) at 200 Hz with an open iris and a shutter speed of
126 $1/600$ s. Two sets of 20 sequentially illuminating LEDs (Wee Beastie Electronics,
127 Loughborough, UK), which were synchronised to the starting signal, were used to synchronise
128 cameras 1 to 4 with the 200 Hz panning camera to within 0.001 s (Irwin & Kerwin, 2006).
129 Camera 5 was subsequently synchronised to camera 4 through calculation of a time offset,
130 which was based on the participants' CM position data from the overlap between cameras 4
131 and 5. First, the time difference between cameras 4 and 5 was determined. Using linear
132 interpolation between two successive CM positions (0.020 s apart) from camera 4, the time at
133 the closest corresponding CM position from camera 5 was estimated. Secondly, the time
134 difference between cameras 4 and 5 was added to the camera 4's synchronisation data from the
135 LED synchronisation lights. This provided the necessary timing data needed to synchronise
136 camera 5 with the 200 Hz panning camera.

137

138 *Data reduction*

139 Videos were manually digitised in Matlab (The MathWorks Inc., USA, version R2014a) using
140 an open source package (DLTdv5, Hedrick, 2008). The data required for calibration were
141 obtained by digitising recordings of a vertical calibration pole with three spherical control
142 points (diameter of 0.100 m) which was moved sequentially through three to five known
143 locations across each camera's field of view (Figure 1). This allowed a $10.00 \text{ m} \times 2.17 \text{ m}$ plane
144 to be calibrated for cameras 1 to 5 using an open source eight parameter 2D-DLT (Meershoek,
145 1997) which was edited to include a ninth parameter to account for lens distortion (Walton,
146 1981). The accuracy of spatial reconstruction was assessed by calculating horizontal and
147 vertical root-mean-squared differences (RMSD) between reconstructed and known points
148 within the calibrated plane. Across both days, reconstruction errors were suitably low, ranging
149 from 0.002 - 0.005 m.

150

151 From the panning camera videos, the touchdown and toe-off events were identified.
152 Touchdown was defined as the first frame when the foot was visibly on the ground, while toe-
153 off was defined as the first frame when the foot was visibly off the ground. The identification
154 of touchdown and toe-off was repeated three times for each trial with at least five days between
155 repetitions. The events identified consistently on at least two separate occasions were used in
156 subsequent processing as the touchdown and toe-off events. Static camera videos were digitised
157 for two frames around each touchdown (last frame before and the first frame of ground contact)
158 and toe-off (last frame before and the first frame of flight) (Bezodis, Kerwin & Salo, 2008).
159 Sixteen body landmarks were digitised: vertex and seventh cervical vertebra (C7), then both
160 hips, shoulders, elbows, wrists, knees, ankles and metatarsophalangeal (MTP) joint centres.
161 Furthermore, the distal end of the contact foot (i.e. the toe) was digitised for three consecutive
162 frames while the foot was on the ground. These three consecutively digitised frames were later
163 averaged during data processing to provide a measure for the position of the front of the shoe
164 during ground contact. To better approximate spatiotemporal data at touchdown and toe-off,
165 event times from the 200 Hz panning camera were synchronised to the data from the static
166 cameras using the LED synch lights (Figure 1) or a least squares fit to the touchdown and toe-off
167 events. Overall, data from all cameras could be synchronised to the nearest 0.002 s. The
168 coordinate positions of each of the digitised points at the 200 Hz touchdown and toe-off events
169 were calculated via linear interpolation between the two frames digitised around touchdown
170 and toe-off.

171

172 To evaluate the reliability of digitising, one trial was re-digitised three times. Variables of
173 interest were calculated from the three sets of digitisations. The absolute and relative (expressed
174 as a percentage of the absolute RMSD relative to variables range across the trial) RMSDs

175 between all re-digitisations were calculated for the variables measured. A relative RMSD below
176 5% was selected as a cut-off for a variable to be deemed reliable. The reliability analysis
177 revealed acceptably low uncertainties with RMSDs of $0.03 \text{ m}\cdot\text{s}^{-1}$ (relative RMSD: 0.6%) for
178 step velocity, between 0.005 - 0.010 m (relative RMSD: 0.0% - 2.9%) for height and distance
179 variables, 0.02 Hz (relative RMSD: 2.0%) for step frequency and between 1° - 2° (relative
180 RMSD: 0.8% - 3.9%) for angular variables. The reliability of the variables was therefore
181 deemed acceptably low to identify step-to-step changes during the sprinting trials.

182

183 *Data processing*

184 The CM at touchdown and toe-off was calculated using segmental inertia data from de Leva
185 (1996) apart from the foot segment for which Winter's (2009) data were used, with the added
186 mass of each athlete's running shoe. Event times, and CM and joint centre locations at
187 touchdown and toe-off were used to calculate the following variables:

188

189 *Sprint Performance [s]*: Time at 50 m minus reaction time. The 50 m time was calculated as
190 the time when the participants' CM reached 50 m, using a fourth-order polynomial, which was
191 fit through all consecutive touchdown and toe-off CM locations from step 1 onwards. Reaction
192 time was determined from the 200 Hz panning camera as the moment when the participants
193 showed the first visible movement in the starting blocks following the start signal.

194

195 *Spatiotemporal variables*: A step was defined from touchdown to the subsequent contralateral
196 touchdown. Step velocity (m/s) was the anteroposterior CM displacement between two
197 consecutive touchdowns divided by the time between the touchdown events. Step length (m)
198 was the anteroposterior displacement of the CM between two consecutive touchdowns, while
199 step frequency (Hz) was the inverse of step time from the panning camera touchdown events.

200 Contact time (s) was calculated by subtracting the touchdown time from the subsequent toe-off
201 time. Flight time (s) was calculated by subtracting the toe-off time from the subsequent
202 touchdown time. Contact distance (m) was calculated as the difference between the
203 anteroposterior positions of the CM at touchdown and subsequent toe-off. Touchdown distance
204 (TD distance, m) was the anteroposterior distance between the MTP and CM at touchdown
205 while toe-off distance (TO distance, m) was the anteroposterior distance between the CM at
206 toe-off and the average toe position during contact. Negative touchdown and toe-off distances
207 represented the CM in front of the contact point. The flight distance (m) was calculated by
208 subtracting the CM position at touchdown from the CM position at the preceding toe-off event.

209

210 *Kinematics:* Segment angles [$^{\circ}$] were defined between the horizontal forward line and the vector
211 created from the distal to proximal segment endpoints. CM, trunk (θ_{trunk}), thigh (θ_{thigh}) and shank
212 (θ_{shank}) angles at touchdown and toe-off were calculated.

213

214 Data from each camera were combined into the full 50 m sprint trial. Since all participants
215 performed at least 25 steps within the 50 m sprint, steps 1-25 were analysed further.

216

217 *Phase identification*

218 Phase identification was based on identifying breakpoint steps at the start of transition (T_{start})
219 and maximal velocity (MV_{start}) phases, respectively. The initial acceleration phase occurred
220 between step one and the step preceding T_{start} , while the transition phase occurred between T_{start}
221 and the step preceding MV_{start} . The maximal velocity phase was defined from MV_{start} to step
222 25. It must be acknowledged that this study will define the maximal velocity phase based on
223 kinematic characteristics generally associated with this phase of the events (i.e. upright posture;
224 e.g. Crick. 2014c) and therefore running velocity may show a small change during this phase.

225 In order to address the first research question, T_{start} and MV_{start} were both identified using
226 multiple approaches.

227

228 T_{start} : This breakpoint step was identified from step-to-step increases in touchdown CM-h (TD
229 CM-h) and touchdown shank angle (TD shank angle). Based on previous literature (e.g.
230 Delecluse et al., 1995; Nagahara et al., 2014b; Crick, 2014b), T_{start} was predicted to occur within
231 the first 10 steps. Therefore, to remove the influence of subsequent data, only the first 10 steps
232 of the sprint were used. A modified method involving multiple straight-line approximation was
233 used to identify T_{start} (see Nagahara et al., 2014b for further details).

234

235 MV_{start} : This breakpoint step was identified based on step-to-step increases in TD CM-h and
236 touchdown trunk angle (TD trunk angle). To remove the influence of data points from the start
237 of the trial, only data from step eight onwards were used (Nagahara et al., 2014b). A method
238 using two first order polynomials was used to identify MV_{start} (see Nagahara et al., 2014b for
239 further details).

240

241 *Data analysis*

242 To address the first research question, and identify breakpoints during maximal sprint
243 acceleration, all trials from both days were used. This allowed a more robust and thorough
244 comparison of the measures used to subdivide the acceleration phase across a range of athletes,
245 trials and sessions. The differences in T_{start} (calculated using either TD CM-h or TD shank
246 angle) and MV_{start} (calculated using either TD CM-h or TD trunk angle) were quantified by
247 calculating an RMSD between respective measures for each participant on each day.

248

249 To address the second research question, each participant's best trial from each day was selected
250 based on 50 m times. This allowed the investigation of the step-to-step technical changes
251 associated with only the best performances from each sprinter in the sample. The measure
252 identified as 'most appropriate' from research question 1 was then used to identify T_{start} and
253 MV_{start} breakpoint steps to address research question 2. T_{start} and MV_{start} breakpoint steps
254 identified from the best trials were used to identify the steps occurring in the initial acceleration,
255 transition and maximal velocity phases of the most successful sprints. Following the
256 identification of T_{start} and MV_{start} , the step-to-step data profiles were smoothed using a Hanning
257 three-point moving averages algorithm (Grimshaw, Fowler, Lees & Burden, 2007).

258

259 Mean step-to-step changes across the steps within the initial acceleration (IAP), transition (TP)
260 and maximal velocity phases (MVP) were calculated for each variable, across each trial.
261 Magnitude-based inferences (MBI; Batterham & Hopkins, 2006) were used to quantify
262 meaningful differences between each participants' mean step-to-step changes between the
263 phases. Differences between means (phases: TP-IAP; MVP-IAP; MVP-TP) were calculated
264 using the post-only crossover spreadsheet (Hopkins, 2006) with a confidence interval (CI) of
265 97%. The smallest worthwhile change was an effect size of 0.2 (Hopkins, 2004; Winter, Abt &
266 Nevill, 2014). Effect sizes were quantified using the following scale: <0.19 (trivial), 0.20-0.59
267 (small), 0.60-1.19 (moderate), 1.20-1.99 (large), 2.00-3.99 (very large) and >4.00 (extremely
268 large; Hopkins, Marshall, Batterham & Hanin, 2009). The probability (percentage and
269 qualitative description) that the differences were larger than 0.20 was defined as; possibly 25-
270 75% (*); likely: 75-95% (**); very likely: 95-99.5% (***) and most likely >99.5% (****;
271 Hopkins et al., 2009). When the outcome of the effect had a >5% chance of being positive and
272 negative, the effect was described as unclear. Median, interquartile range and range of

273 step-to-step changes within each phase were calculated across all ten trials and presented in box
274 and whisker plots.

275

276 **Results**

277 Ranges of performance (50 m time) and the identified breakpoint steps are presented in Table
278 2. Only P1 (6.13-6.07 s) and P3 (5.90-5.89 s) improved on their best performance from day 1
279 to 2. The RMSD between T_{start} identified using TD CM-h or TD shank angles ranged from 0.8-
280 2.1 steps, whilst the RMSD between MV_{start} identified using TD CM-h or TD trunk angles
281 ranged from 1.3-2.3 steps (Table 2). The within-participant ranges of T_{start} steps identified
282 averaged 1.9 steps using TD CM-h and 2.2 steps using TD shank angles. Ranges of MV_{start}
283 steps identified averaged 2.8 steps using TD CM-h and 2.6 steps using TD trunk angles.

284

285 ****Insert table 2 near here****

286

287 To address the second research question, the ranges of T_{start} and MV_{start} steps based on the
288 step-to-step changes in TD CM-h were identified from each participants' best trials and used to
289 sub-divide the whole 50 m sprint into three distinct phases, which had no possible overlap (see
290 shaded areas on Figures 2-4). The initial acceleration phase therefore comprised steps one to
291 three, the transition phase steps six to 13, and the maximal velocity phase steps 17 to 25. T_{start}
292 was associated with step velocities of 6.06 to 7.83 m/s (65 to 77% V_{max} , which was 8.86 to
293 10.73 m/s), while the MV_{start} was associated with step velocities of 8.19 to 10.07 m/s (92 to
294 98% V_{max}).

295

296 Over the 25 steps, the largest step-to-step changes in step velocity, step length and step
297 frequency (Figure 2) occurred during the initial acceleration phase (i.e. steps 1 to 3), with

298 extremely large step-to-step increases in step velocity and step length and trivial to very large
299 step-to-step increases in frequency compared to the transition and maximal velocity phases.
300 During the transition phase, mean step-to-step increases in step velocity were extremely large,
301 mean increases in step length were large to very large and mean changes in step frequency were
302 trivial to small compared to the maximal velocity phase.

303

304 ****Insert figure 2 near here****

305

306 The initial acceleration phase was characterised by small to very large changes in contact times,
307 flight times, contact distances, flight distances and touchdown distance compared to the
308 transition and maximal velocity phases (Figure 3). During the transition phase, step-to-step
309 changes in contact distances (Figure 3e) plateaued or started decreasing as increases in
310 touchdown distances (0.01 to 0.02 m per step; Figure 3m&n) were equal to or smaller than
311 decreases in toe-off distances (0.01 to 0.03 m per step; Figure 3o&p). During the maximal
312 velocity phase, flight times and flight distances continued to show small step-to-step increases.
313 Mean step-to-step increases in touchdown and toe-off CM-h were very large to extremely large
314 between the initial acceleration and the transition phases and small to large between the
315 transition and maximal velocity phases.

316

317 ****Insert figure 3 near here****

318

319 Step-to-step changes in touchdown CM-angle were most likely large to very large between the
320 initial acceleration phase and both later phases, but most likely only small between the transition
321 and maximal velocity phases (Figure 4). Changes in toe-off CM-angle were most likely

322 moderate to very large between the maximal velocity phase and both preceding phases, and
323 very likely small to very large between the initial acceleration and transition phases.

324

325 ****Insert figure 4 near here****

326

327 **Discussion and Implications**

328 Increased understanding of the technical changes associated with different phases in sprinting
329 is important to facilitate the development of technical models of sprinting. Therefore, the aim
330 of this study was to investigate spatiotemporal and kinematic changes between the initial
331 acceleration, transition and maximum velocity phases of a sprint. To address this aim, two
332 research questions were developed.

333

334 Firstly, to compare different measures previously proposed in scientific (Nagahara et al., 2014b)
335 and coaching literature (Crick 2014a), the first research question - '*how comparable are the*
336 *sprint acceleration phases when identified using different measures?*' was addressed. The
337 within-trial RMSD analysis revealed differences up to 2.3 steps between for the T_{start} and MV_{start}
338 steps identified using the different variables. Hypothesis a) that the sprint acceleration phases
339 identified using changes in TD CM-h will align with the phases identified using shank and trunk
340 angles was therefore rejected. Although relatively low, these RMSD step differences are
341 ultimately due to other segments than the shank and trunk changing independently and therefore
342 influencing the TD CM-h. Furthermore, bilateral differences, which have previously been
343 reported in maximal sprinting (Exell, Gittoes, Irwin & Kerwin, 2012) could have contributed
344 to these RMSD step differences. While the within-trial analysis revealed that different T_{start} and
345 MV_{start} steps were identified when using either TD CM-h or touchdown segments angles, both
346 measures did provide similar ranges of T_{start} and MV_{start} steps across multiple trials. Therefore,

347 using segment angles in applied settings, where the speed of feedback is often an important
348 factor may be an appropriate substitute provided that these data are based on multiple trials (at
349 least three trials per participant). However, since TD CM-h provides a more robust and holistic
350 measure that is more representative of the overall postural changes and changes in CM
351 acceleration, this measure is more appropriate for identifying T_{start} and MV_{start} and was therefore
352 subsequently used to address research question 2.

353

354 To understand technical differences between phases, the second research question – ‘*how do*
355 *step-to-step progressions of spatiotemporal and kinematic variables differ between the initial*
356 *acceleration, transition and maximal velocity phases?*‘ was examined. Using TD CM-h, steps
357 one to three were defined as the initial acceleration phase, steps 6-13 the transition phase, and
358 steps 17-25 the maximal velocity phase. Standardised differences in mean between-step
359 increases of the CM-angle between the initial acceleration and transition phases were very large
360 (ES confidence interval: 1.30 to 3.80) for touchdown angles and large (ES confidence interval:
361 0.33 to 2.31) for toe-off angles. Comparing the transition and maximal velocity phases,
362 standardised differences in mean step-to-step increases of CM-angles were small (ES
363 confidence interval: 0.27 to 0.53) for touchdown angles and very large (ES confidence interval:
364 1.16 to 2.14) for toe-off angles. Based on this, hypothesis b) that there will be large differences
365 in step-to-step changes of CM-angle between the initial acceleration, transition and maximal
366 velocity phases, was only partially accepted. These changes in touchdown and toe-off CM-
367 angles provide some important insight into the initial acceleration and transition phases.

368

369 The more forward-inclined orientation of the participants (i.e. smaller touchdown and toe-off
370 CM-angles; Figure 4a&c) during the initial acceleration phase compared to the transition phase
371 is indicative of the capacity to generate larger net anteroposterior forces (Kugler & Janshen,

2010; Rabita et al., 2015) during this phase. This explains the extremely large step-to-step increases in step velocity during initial acceleration (median 0.88 m/s per step; Figure 2a&b) compared to the transition phase (median 0.24 m/s per step). Additionally, these extremely large increases in step velocity during the initial acceleration phase were achieved through extremely large increases in step length and trivial to very large increases in step frequency, compared to the transition phase. Previous research has reported that across a group of sprinters, performance during the initial acceleration phase is dependent on large increases in step frequency (Nagahara et al., 2014a) and that within athletes, better performances were influenced by larger magnitudes of step frequency throughout the acceleration phase (Nagahara, Mizutani, Matsuo, Kanehisa & Fukunaga, 2018b). Ultimately, the magnitude of the step frequency, which is determined by the sum of contact and flight times, is an important determinant of step velocity. The ability to quickly increase step frequency during the initial acceleration phase (Debaere, Jonkers, & Delecluse, 2013; Nagahara et al., 2014a) may be an important characteristic of this phase compared to the transition and maximal velocity phases. In the current study, the large step-to-step increases in step frequency (median 0.12 steps·s⁻¹ per step; Figure 3a&b) during the initial acceleration phase were due to larger decreases in contact times (median -0.020 s per step; Figure 3a&b) relative to the increases in flight times (median 0.012 s per step; Figure 3a&b). As contact times are related to running velocity (Hunter et al., 2004), shorter contact times are dependent on larger running velocities which can be achieved by applying larger propulsive impulses during preceding steps (Nagahara et al., 2018b). Therefore, as a sprinter's ability to generate larger propulsive forces during the initial acceleration phase increases, their larger change in running velocity will result in larger decreases in contact times which could allow them to achieve larger increases in step frequency.

396 During the transition phase, further increases in step velocity were mainly due to step-to-step
397 increases in step length, which in turn resulted from further increases in flight distance (Figure
398 3g). Previous research has demonstrated that flight distance is determined by the anterior and
399 vertical CM velocity at toe-off, the latter of which is also the main determinant of flight time
400 (Hunter et al., 2004). Therefore, as step velocities increase, sprinters need to increase the
401 magnitude of vertical force production to facilitate a decrease in contact times (Figure 3a)
402 without impeding step-to-step increases in CM-h (Figure 3i) and flight times (Figure 3c).
403 However, since a more forward-inclined GRF vector (Rabita et al., 2015; Nagahara, Mizutani,
404 Matsuo, Kanehisa & Fukunaga, 2018a) and a smaller vertical impulse predicts better
405 acceleration performance (Nagahara et al., 2018a), there likely exists an ideal magnitude of
406 vertical force that facilitates increases in step velocity without negatively affecting step
407 frequency through excessively long flight times.

408

409 Segmental changes that influence changes in CM-angle can provide an insight into how
410 sprinters adjust force production. During the initial acceleration phase, the relatively large
411 step-to-step increases in touchdown CM-angle, compared to the transition phase, were
412 influenced by increases in shank (median 9° per step) and trunk angles (median 4° per step).
413 These results align with the coaching literature, which suggests that during the initial
414 acceleration phase, experienced sprinters show step-to-step changes in shank angles of between
415 6 to 8° per step (Crick, 2014b). These increased touchdown variables during the initial
416 acceleration phase could ultimately contribute to the decrease in the anterior forces sprinters
417 can generate during subsequent ground contacts. This may be due to the increases in shank and
418 trunk angles and could result in larger touchdown distances, which have been previously linked
419 to larger braking forces (Hunter, Marshall & McNair, 2005). Additionally, the relatively large
420 step-to-step increases in CM-h (Figure 3i&k) and trunk angles (Figure 4e&g) during the initial

421 acceleration phase could influence the increasing toe-off CM-angles (Figure 4c) and therefore
422 the capacity to generate large propulsive forces (e.g. di Prampero et al., 2005; Kugler &
423 Janshen, 2010). Although a decreased touchdown distance has been shown to be beneficial
424 during the first step of a sprint (Bezodis, Trewartha & Salo, 2015), the large magnitude of
425 step-to-step increases in TD variables may ultimately reflect a requirement to generate larger
426 magnitudes of vertical force and therefore flight times (Figure 3c) as a sprint progresses.
427 Previous research from the maximal velocity phase of sprinting suggested that sprinters
428 generate larger vertical forces early during ground contact due to their upright trunk and
429 extended hip and knee joint, which provide increased stiffness at touchdown (Clark & Weyand,
430 2014). Similarly, during earlier sprint phases, the increasing TD CM-angle (Figure 4a), TD
431 CM-h (Figure 3i) and more extended hip and knee joints due to the increasing TD trunk (Figure
432 4e) and shank (Figure 4m) angles could increase the capacity to generate vertical force early
433 during ground contact and therefore minimise the loss in CM-h immediately following
434 touchdown.

435

436 At toe-off, the CM-angle increased during both the initial acceleration (median 2° per step;
437 Figure 4c&d) and transition phases (median 1° per step; Figure 4c&d). Although smaller CM-
438 angles at toe-off could facilitate larger propulsive force production (Kugler & Janshen, 2010),
439 the step-to-step increases in toe-off CM-angle may be unavoidable given the increases in
440 touchdown CM-angles, CM-h, trunk angles and decreases in contact times. Coaching literature
441 proposed trunk angle and changes in trunk angle as important factors influencing anterior force
442 production during sprinting (Crick, 2014c), and suggested that better sprinters likely show
443 smaller step-to-step increases in trunk angles (Crick, 2014c). Ultimately, the increasing trunk
444 angle (Figure 4e&g) during the initial acceleration and transition phases may play an important
445 role in influencing the toe-off CM-angle by limiting the anterior rotation of the thigh (Figure

446 4k) and therefore contribute to the increases in toe-off distances (Figure 3e). This could
447 ultimately contribute to the decreasing magnitude of propulsive forces sprinters can generate as
448 a sprint progresses (e.g. Nagahara et al., 2018a).

449

450 Compared to the initial acceleration and transition phases, the maximal velocity phase was
451 characterised by small to negligible step-to-step changes in many spatiotemporal (Figure 2&3)
452 and kinematic variables (Figure 4). At MV_{start} , participants had reached 92-98% of maximal
453 velocity. These results show parity with the British Athletics technical model, which suggests
454 that world-class sprinters reached 95% of maximal velocity at MV_{start} (Crick, 2014c). The
455 participants still showed small increases in step velocity (Figure 2a) which suggests that the
456 participants maintained a positive net anterior impulse during the maximal velocity phase. This
457 was further reflected in the small increases in flight distances (Figure 3g) and therefore step
458 lengths (Figure 2c) which continued throughout the maximal velocity phase. This supports the
459 results by Ae, Ito, and Suzuki (1992) who reported that step length increases continue
460 throughout a sprint. These results could be explained by the upright trunk and high knee lift,
461 which are associated with this phase of sprinting and allow sprinters a longer path to accelerate
462 their foot down and backwards prior to touchdown. This would contribute to increasing vertical
463 force production earlier during ground contact (Clark & Weyand, 2014) and reduced braking
464 forces (Hunter et al., 2005). The upright posture of sprinters is thought to benefit the mechanics
465 during late swing and early ground contact (i.e. 'front side mechanics'; Mann, 2007, p. 86) and
466 vertical force production (e.g. Clark & Weyand, 2014) during the maximal velocity phase.
467 However, the increasing trunk angle as a sprint progresses might provide an unavoidable
468 constraint limiting toe-off distances and therefore the magnitude of propulsive forces sprinters
469 can theoretically generate. Therefore, as a sprint progresses through the initial acceleration,

470 transition and maximal velocity phases, sprinters may have a greater ability to manage
471 touchdown rather than toe-off mechanics in an attempt to influence performance.

472

473 Despite having five participants in this study, the parity of the results with previous scientific
474 and coaching literature as well as the between-participant consistency regarding the step-to-step
475 changes in the different variables provides confidence in the applicability of this data to
476 investigate changes associated with maximal sprinting. The results presented in the current
477 study provide important insights to increase understanding of the differences between phases
478 in maximal sprinting. Overall, the changing spatiotemporal and kinematic variables through the
479 different phases have important implications for the performance of the sprinters. The changes
480 in CM-h and CM-angle suggest that participants increased vertical force production through
481 changes in touchdown mechanics, while changes in toe-off mechanics suggest an unavoidable
482 limiting feature that dictates decreases in propulsive force production as a sprint progresses.
483 Finally, while breakpoints were identified to define the initial acceleration, transition and
484 maximal velocity phases, this study did not investigate how differences in the location of the
485 breakpoint steps between different trials were associated with differences in spatiotemporal and
486 kinematic variables. While the aim of this study was to investigate differences between the
487 phases of a sprint, an investigation of how changes in breakpoints are related to spatiotemporal
488 and kinematic variables may represent a future avenue of research.

489

490 **Conclusions**

491 The current study has developed an understanding of the technical changes associated with the
492 different phases of a maximal sprint. As long as a sufficient number of trials are available for
493 analysis (at least three), using shank and trunk angles may represent an appropriate measure to
494 detect breakpoint steps in applied settings. However, CM-h represents a more holistic measure

495 of overall postural changes, which links to the centre of mass acceleration, and therefore
496 provides a more robust measure to identify phases during maximal sprinting. This analysis
497 revealed important changes in whole body posture that may be linked to force production,
498 which would ultimately determine the increases in step velocity associated with the initial
499 acceleration phase compared to the transition and maximal velocity phases. These results
500 provide coaches and practitioners with valuable insights into key differences between phases in
501 maximal sprinting.

502

503 **References**

504 Ae, M., Ito, A. & Suzuki, M. (1992). The men's 100 metres. *New Studies in Athletics*, 7(1), 47-
505 52.

506

507 Batterham, A. M., & Hopkins, W. G. (2006). Making meaningful inferences about
508 magnitudes. *International Journal of Sports Physiology and Performance*, 1(1), 50-57. doi:
509 10.1123/ijsp.1.1.50.

510

511 Bezodis, I. N., Kerwin, D. G., & Salo, A. I. (2008). Lower-limb mechanics during the support
512 phase of maximum-velocity sprint running. *Medicine and Science in Sports and Exercise*,
513 40(4), 707-715. doi: 10.1249/MSS.0b013e318162d162

514

515 Bezodis, N. E., Trewartha, G., & Salo, A. I. T. (2015). Understanding the effect of touchdown
516 distance and ankle joint kinematics on sprint acceleration performance through computer
517 simulation. *Sports Biomechanics*, 14(2), 232-245. doi: 10.1080/14763141.2015.1052748

518

519 Clark, K. P., & Weyand, P. G. (2014a). Are running speeds maximized with simple-spring
520 stance mechanics?. *Journal of Applied Physiology*, 117(6), 604-615. doi:
521 10.1152/jappphysiol.00174.2014
522

523 Čoh, M. & Tomazin, K. (2006). Kinematic analysis of the sprint start and acceleration from
524 the blocks. *New Studies in Athletics* 21(3), 23-33.
525

526 Crick, T. (2014a, November 9). Understanding the performance profiles of sprint events
527 [PDF]. Retrieved from <http://ucoach.com/>
528

529 Crick, T. (2014b, November 9). The Drive Phase. [PDF]. Retrieved from <http://ucoach.com/>
530

531 Crick, T. (2014c, November 9). The Transition, Max Velocity and Speed Maintenance
532 Phases. [PDF]. Retrieved from <http://ucoach.com/>
533

534 de Leva, P. (1996). Adjustments to Zatsiorsky-Seluyanov's segment inertia parameters.
535 *Journal of Biomechanics*, 29(9), 1223-1230. doi: 10.1016/0021-9290(95)00178-6
536

537 Debaere, S., Jonkers, I., & Delecluse, C. (2013). The contribution of step characteristics to
538 sprint running performance in high-level male and female athlete. *Journal of Strength and*
539 *Conditioning Research*, 27(1), 116-124. doi: 10.1519/JSC.0b013e31825183ef
540

541 Delecluse, C., Van Coppenolle, H., Diels, R., & Goris, M. (1992). A model for the scientific
542 preparation of high level sprinters. *New Studies in Athletics*, 7(4), 57-64.
543

544 Delecluse, C.H., Van Coppenolle, H., Willems, R., Diels, M., Goris, M., Van Leemputte, M.,
545 & Vuylsteke, M. (1995). Analysis of the 100 meter Sprint performance as a multi-
546 dimensional skill. *Journal of Human Movement Studies*, 28, 87-101.

547

548 Delecluse, C. (1997). Influence of strength training on sprint running performance. *Sports*
549 *Medicine*, 24(3), 147 – 156.

550

551 di Prampero, P. E., Fusi, S., Sepulcri, L., Morin, J. B., Belli, A., & Antonutto, G. (2005).
552 Sprint running: a new energetic approach. *Journal of Experimental Biology*, 208(14), 2809-
553 2816. doi: 10.1242/jeb.01700

554

555 Dick, F. W. (1989). Development of maximum sprinting speed. *Track Coach*, 109, 3475-
556 3480.

557

558 Exell, T. A., Irwin, G., Gittoes, M. J., & Kerwin, D. G. (2012). Implications of intra-limb
559 variability on asymmetry analyses. *Journal of Sports Sciences*, 30(4), 403-409. doi:
560 10.1080/02640414.2011.647047

561

562 Grimshaw, P., Fowler, N., Lees, A., & Burden, A. (2007). Sport and exercise biomechanics
563 (1st ed., pp. 312-316). Abingdon, Oxon: Taylor & Francis Group.

564

565 Hedrick, T. L. (2008). Software techniques for two-and three-dimensional kinematic
566 measurements of biological and biomimetic systems. *Bioinspiration & Biomimetics*, 3(3).
567 034001. doi: 10.1088/1748-3182/3/3/034001.

568

569 Hopkins, W. G. (2004). How to interpret changes in an athletic performance test.
570 *Sportscience*, 8, 1–7. Retrieved from sportssci.org/jour/04/wghtests.htm
571

572 Hopkins W.G. (2006). Spreadsheets for analysis of controlled trials with adjustment for a
573 predictor. *Sportscience*, 10, 46-50. Retrieved from sportssci.org/2006/wghcontrial.htm
574

575 Hopkins, W., Marshall, S., Batterham, A., & Hanin, J. (2009). Progressive statistics for
576 studies in sports medicine and exercise science. *Medicine and Science in Sports and Exercise*,
577 41(1), 3-13. doi: 10.1249/MSS.0b013e31818cb278
578

579 Hunter, J. P., Marshall, R.N., & McNair, P. J. (2004). Interaction of Step Length and Step
580 Rate during Sprint Running. *Medicine & Science in Sports & Exercise*, 36(2), 261–271.
581

582 Hunter, J. P., Marshall, R. N., & McNair, P. J. (2005). Relationships between ground reaction
583 force impulse and kinematics of sprint-running acceleration. *Journal of applied*
584 *biomechanics*, 21(1), 31-43.
585

586 Irwin, G. and Kerwin, D.G. (2006). Musculoskeletal work in the longswing on high bar. In:
587 E.F. Moritz and S. Haake (eds.), *The Engineering of Sport 6 Volume 1: Developments for*
588 *Sports* (pp. 195-200). New York: Springer LLC.
589

590 Kugler, F., & Janshen, L. (2010). Body position determines propulsive forces in accelerated
591 running. *Journal of biomechanics*, 43(2), 343-348.
592

593 Mann, R. (2007). *The Mechanics of Sprinting and Hurdling*. Las Vegas, NV: Author.

594 Meershoek, L. (1997). Matlab routines for 2-D camera calibration and point reconstruction
595 using the DLT for 2-D analysis with non-perpendicular camera angle [online]. Retrieved from
596 <https://isbweb.org/software/movanal.html>
597

598 Nagahara, R., Naito, H., Morin, J. B., & Zushi, K. (2014a). Association of acceleration with
599 spatiotemporal variables in maximal sprinting. *International journal of sports*
600 *medicine*, 35(9), 755-761. doi: 10.1055/s-0033-1363252
601

602 Nagahara, R., Matsubayashi, T., Matsuo, A., & Zushi, K. (2014b). Kinematics of transition
603 during human accelerated sprinting. *Biology Open*, 3(8), 689–699. doi: 10.1242/bio.20148284
604

605 Nagahara, R., Mizutani, M., & Matsuo, A. (2016, July). Ground reaction force of the first
606 transition during accelerated sprinting: a pilot study. In: M. Ae, Y. Enomoto, N. Fujii, & H.
607 Takagi (Eds.), *ISBS 2016. Proceedings of the 34rd International Conference on Biomechanics*
608 *in Sports* (pp. 859-862). Tsukuba, Japan
609

610 Nagahara, R., Mizutani, M., Matsuo, A., Kanehisa, H., & Fukunaga, T. (2018a). Association
611 of sprint performance with ground reaction forces during acceleration and maximal speed
612 phases in a single sprint. *Journal of Applied Biomechanics*, 34(2), 104-110. doi:
613 10.1123/jab.2016-0356.
614

615 Nagahara, R., Mizutani, M., Matsuo, A., Kanehisa, H., & Fukunaga, T. (2018b). Step-to-step
616 spatiotemporal variables and ground reaction forces of intra-individual fastest sprinting in a
617 single session. *Journal of Sports Sciences*, 36(12), 1392-1401. doi:
618 10.1080/02640414.2017.1389101

619 Rabita, G., Dorel, S., Slawinski, J., de Villarreal, E. S., Couturier, A., Samozino, P., & Morin,
620 J. B. (2015). Sprint mechanics in world-class athletes: a new insight into the limits of human
621 locomotion. *Scandinavian Journal of Medicine & Science in Sports*, 25(5), 583-594. doi:
622 10.1111/sms.12389

623

624 Seagrave, L. (1996). Introduction to sprinting. *New Studies in Athletics*, 11(2), 93- 113.

625

626 Volkov, N. I., & Lapin, V. I. (1979). Analysis of the velocity curve in sprint running.
627 *Medicine and Science in Sports and Exercise*, 11(4), 332-337. doi: 10.1249/00005768-
628 197901140-00004

629

630 Walton, J. (1981). *Close-range cine-photogrammetry: A generalised technique for*
631 *quantifying gross human motion*. Unpublished Doctoral Thesis. The Pennsylvania State
632 University.

633

634 Winter, D.A. (2009). *Biomechanics and Motor Control of Human Movement* (4th Edition, p.
635 86). Hoboken, NJ: John Wiley and Sons, Inc.

636

637 Winter, E. M., Abt, G. A., & Nevill, A. M. (2014). Metrics of meaningfulness as opposed to
638 sleights of significance. *Journal of Sports Sciences*, 32(10), 901– 902.
639 doi:10.1080/02640414.2014.895118

640

641

642

643

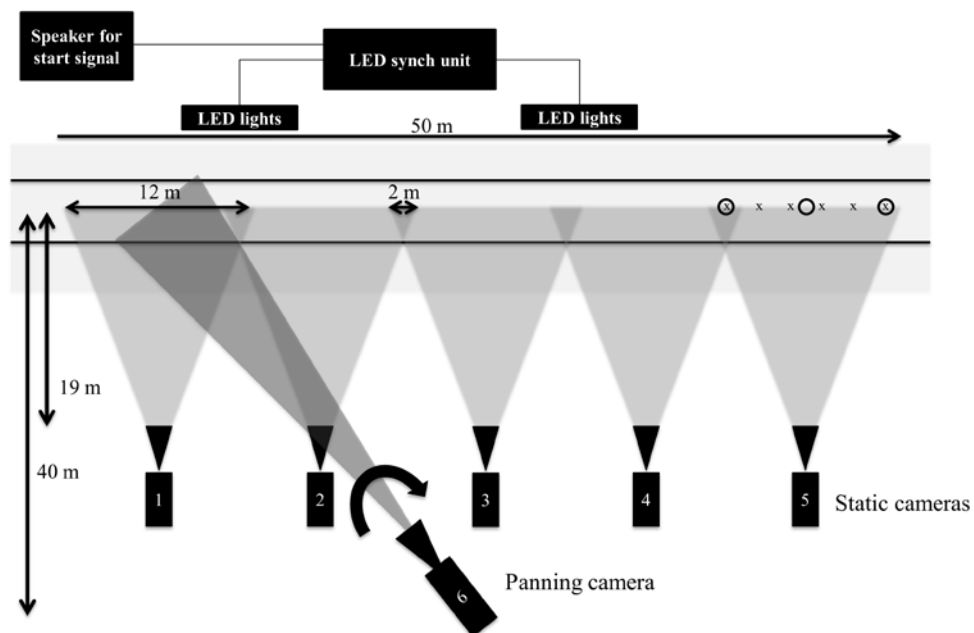
Table 1. Participant characteristics.

ID	Age	Gender	Stature [m]	Body Mass [kg]	60 m/100 m PB [s]
P1	27	Male	1.89	89.1	6.99/10.87
P2	20	Male	1.79	73.5	6.80/10.64
P3	19	Male	1.79	72.0	6.86/10.71
P4	20	Female	1.76	69.4	7.65/12.34
P5	25	Female	1.71	63.3	7.61/11.90

Table 2. Ranges of performance times, maximal step velocities and breakpoint steps identified for each participant on each day. RMSD values are presented between T_{start} steps identified using either TD CM-h or TD shank angles, and between MV_{start} steps identified using either TD CM-h or TD trunk angles. Data are based on all available trials for each participant.

Participant	Day	50 m time (s)	Range of maximum Step Velocities (m/s)	T_{start}			MV_{start}		
				TD CM-h	TD θ_{shank}	TD CM-h vs. TD θ_{shank}	TD CM-h	TD θ_{trunk}	TD CM-h vs. TD θ_{trunk}
P1	1	6.13 – 6.21	9.59 – 9.93	5-7	3-6	1.6	14-17	15-18	1.3
	2	6.07 – 6.15	9.82 – 10.20	3-5	3-6	1.5	13-17	15-17	1.4
P2	1	5.86 – 5.94	10.53 – 10.76	3-5	3-5	1.2	14-15	14-16	1.6
	2	5.98 – 6.01	10.35 – 10.56	3-6	3-6	0.8	13-15	12-16	2.0
P3	1	5.90 – 5.96	10.53 – 10.61	3-4	3-6	2.1	15-17	17-18	2.3
	2	5.89 – 5.94	10.40 – 10.63	4-5	4-6	1.3	14-17	14-17	1.3
P4	1	6.78 – 6.90	8.83 – 9.04	3-5	5	1.1	12-17	14-15	1.6
	2	6.83 – 7.06	8.56 – 8.86	5-6	3-5	1.1	13-16	14-19	1.7
P5	1	6.63 – 6.75	8.99 – 9.15	4-7	4-6	1.1	14-16	13-17	2.0
	2	6.75 – 6.78	8.96 – 9.10	5-7	4-6	0.9	14-17	13-15	1.7
All	1			3-7	3-6	1.5	12-17	13-18	1.8
	2			3-7	3-6	1.1	13-17	12-19	1.7

Note: SV: step velocity, TD CM-h: touchdown centre of mass height, TD θ_{shank} : touchdown shank angles, TD θ_{trunk} : touchdown trunk angles, T_{start} : step representing the start of the transition phase, MV_{start} : step representing the start of the maximal velocity phase.

**Figure 1.** Camera and synchronisation light set-up (not to scale). An example of the camera calibration points for days 1 (O) and 2 (X) are shown in camera 5's field of view. This was repeated for all five static cameras. The direction of travel was from left to right.

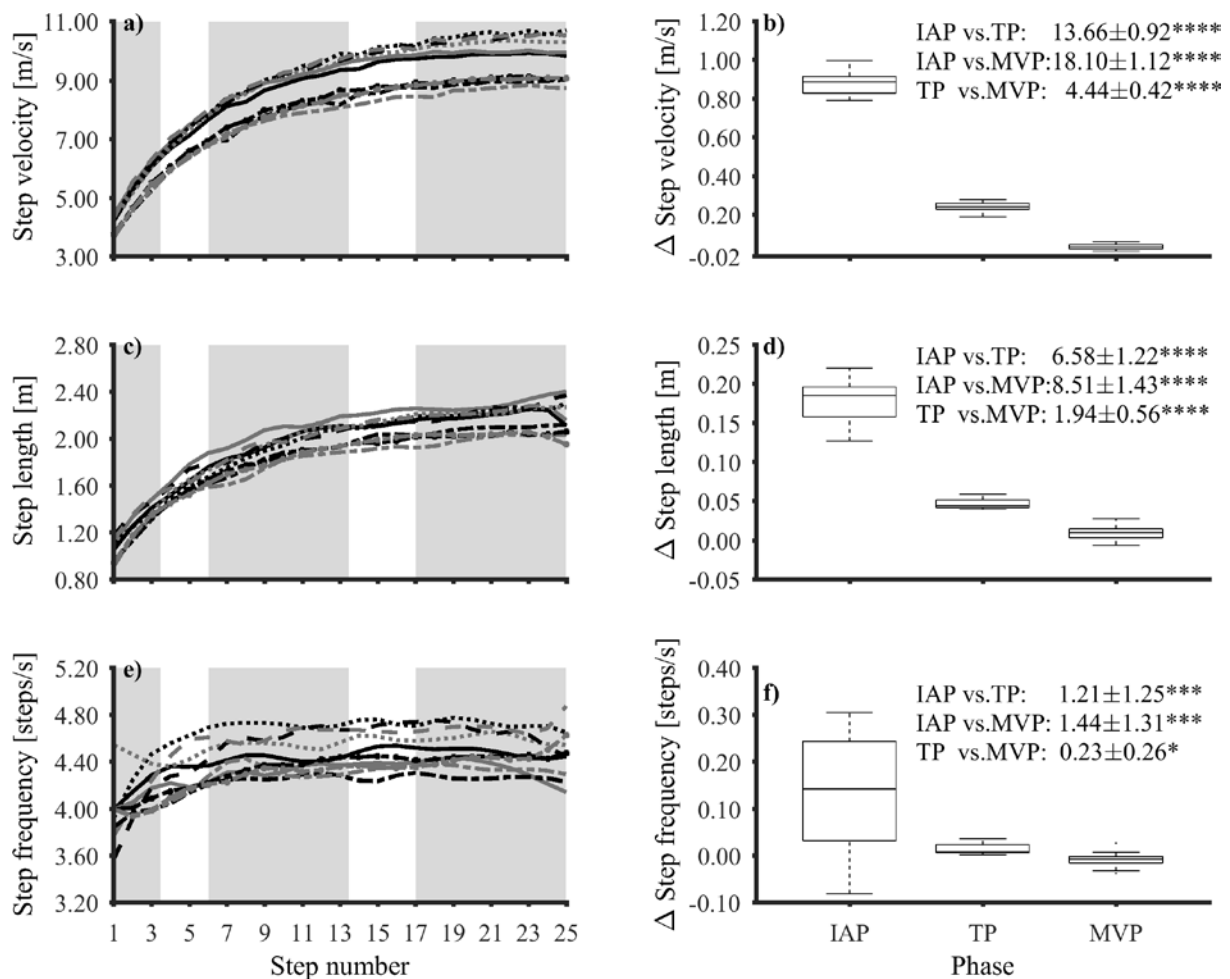


Figure 2. Step-to-step step velocity (a), step length (c) and step frequency (e) profiles of the participants' best 50 m sprints from day 1 (black) and day 2 (grey). Each participant is represented by particular line style. Grey columns highlight the initial acceleration, transition and maximal velocity phases. Box and whisker plots, figures b, d, f show the median, interquartile range and range of between step changes during the initial acceleration, transition and maximal velocity phases. Magnitude-based inference results presented on figures b, d and f show the mean standardised effect \pm 97% confidence interval. The probability that the differences were bigger than the smallest worthwhile change (i.e. 0.20) was defined by: unclear (no stars), possibly (*); likely (**); very likely (***) and most likely (****).

646

647

648

649

650

651

652

653

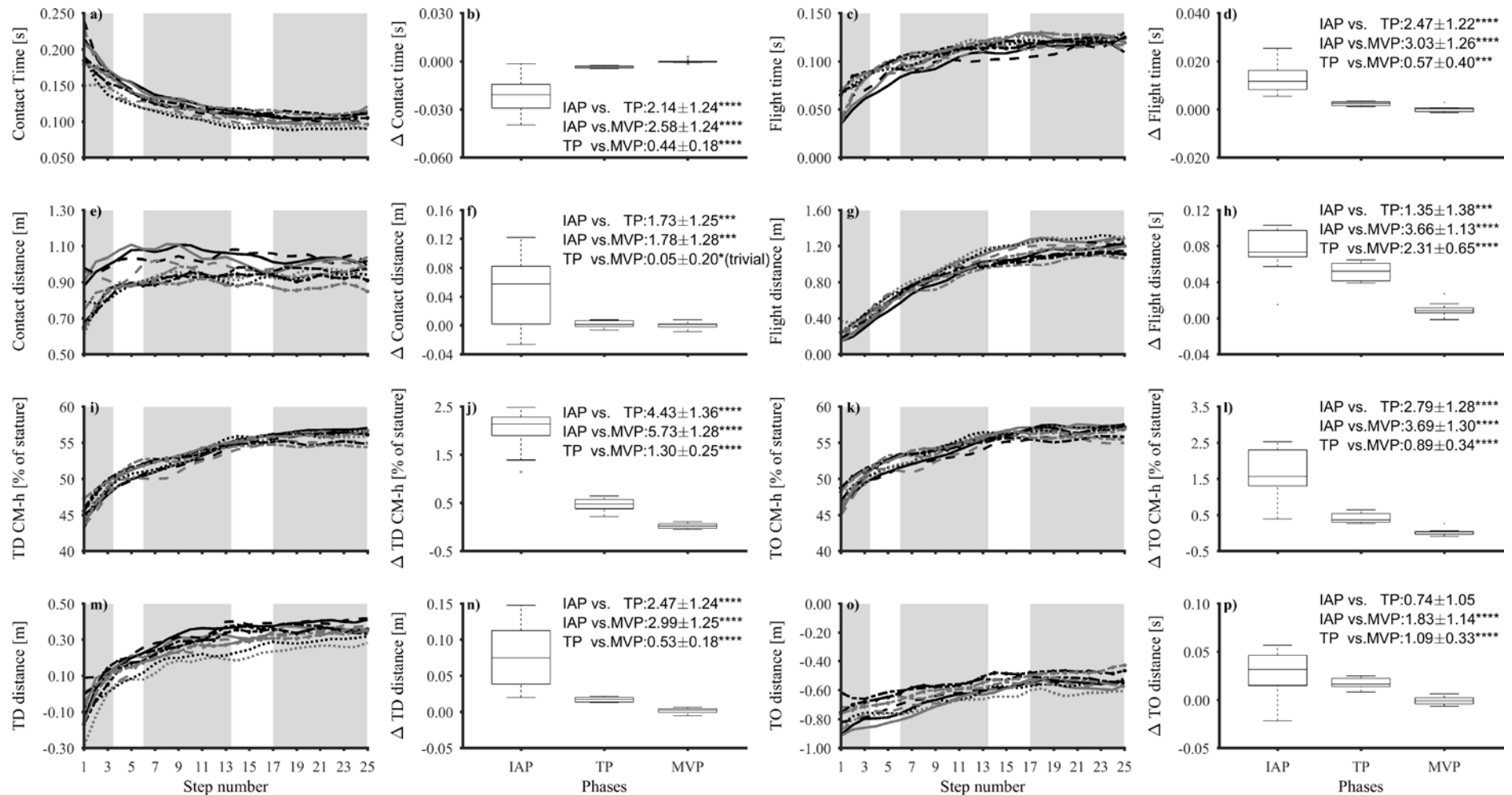


Figure 3. Step-to-step contact times (a), flight times (c), contact distance (e), flight distance (g), TD CM-h (i), TO CM-h (k), TD distance (m) and TO distances (o) profiles of the participants best 50 m sprint from day 1 (black) and day 2 (grey). Each participant is represented by particular line style. Grey columns highlight the initial acceleration, transition and maximal velocity phases. Box and whisker plots, figures b, d, f, h, j, l, n and p show the median, interquartile range and range of between step changes during the initial acceleration, transition and maximal velocity phases. Magnitude-based inference results presented on figures b, d, f, h, j, l, n and p show the mean standardised effect \pm 97% confidence interval. The probability that the differences were bigger than the smallest worthwhile change (i.e. 0.20) was defined by: unclear (no stars), possibly (*); likely (**); very likely (***) and most likely (****).

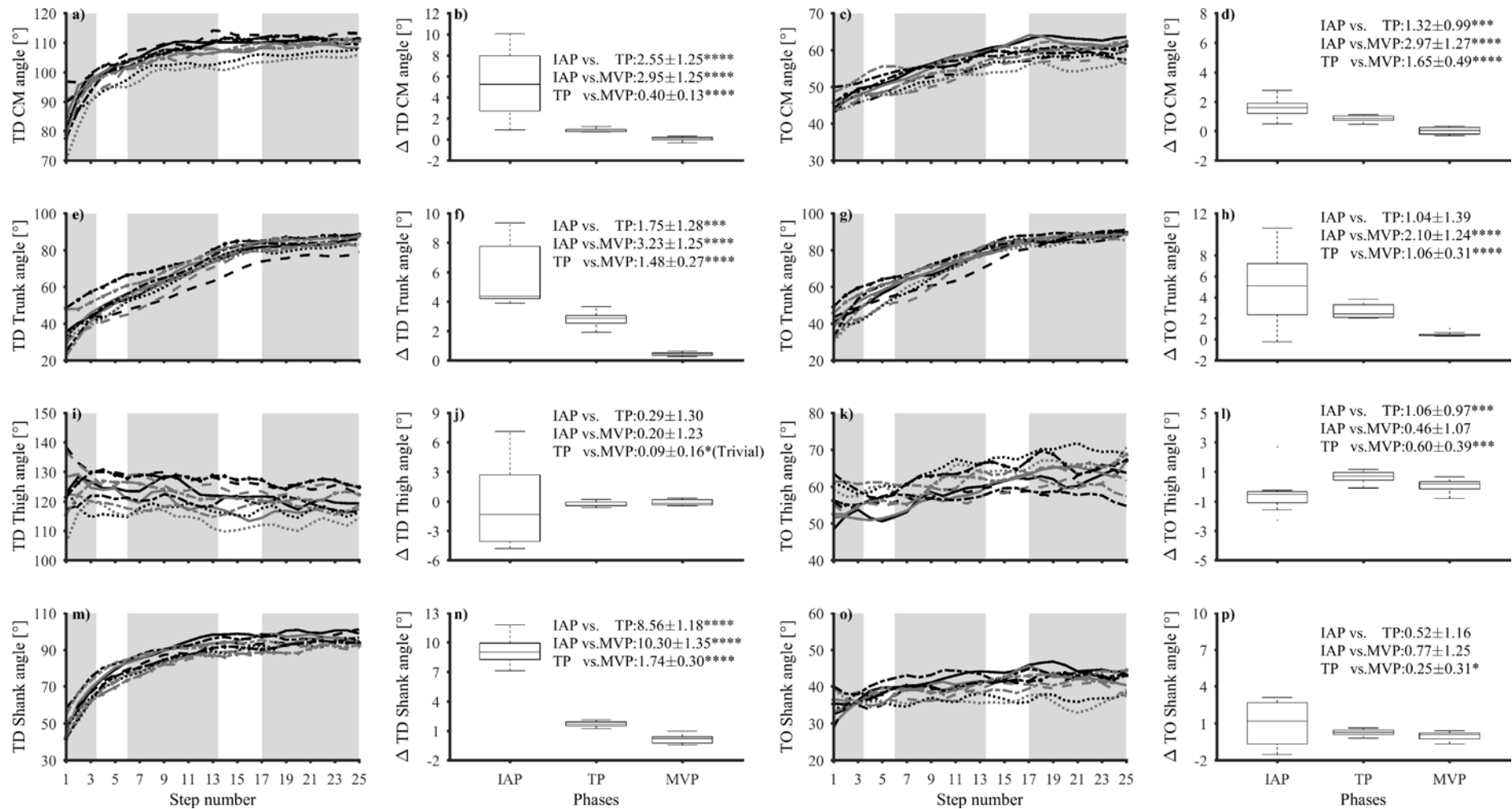


Figure 4. Step-to-step TD CM-angle (a), TO CM-angle (c), TD trunk angle (e), TO trunk angle (G), TD thigh angle (i), TO thigh angle (k), TD shank angle (m) and TO shank angle (o) profiles of the participants best 50 m sprints from days 1 (black) and 2 (grey). Each participant is represented by particular line style. Grey columns highlight the initial acceleration, transition and maximal velocity phases. Box and whisker plots, figures b, d, f, h, j, l, n and p show the median, interquartile range and range of between step changes during the initial acceleration, transition and maximal velocity phases. Magnitude-based inference results presented on figures b, d, f, h, j, l, n and p show the mean standardised effect \pm 97% confidence interval. The probability that the differences were bigger than the smallest worthwhile change (i.e. 0.20) was defined by: unclear (no stars), possibly (*); likely (**); very likely (***) and most likely (****).